ACCOUNTS
of chemical research

Controlling Transport and Chemical Functionality of Magnetic Nanoparticles

ANDREW H. LATHAM AND MARY ELIZABETH WILLIAMS*

Department of Chemistry, The Pennsylvania State University, 104 Chemistry Building, University Park, Pennsylvania 16802

RECEIVED ON AUGUST 7, 2007

CONSPECTUS

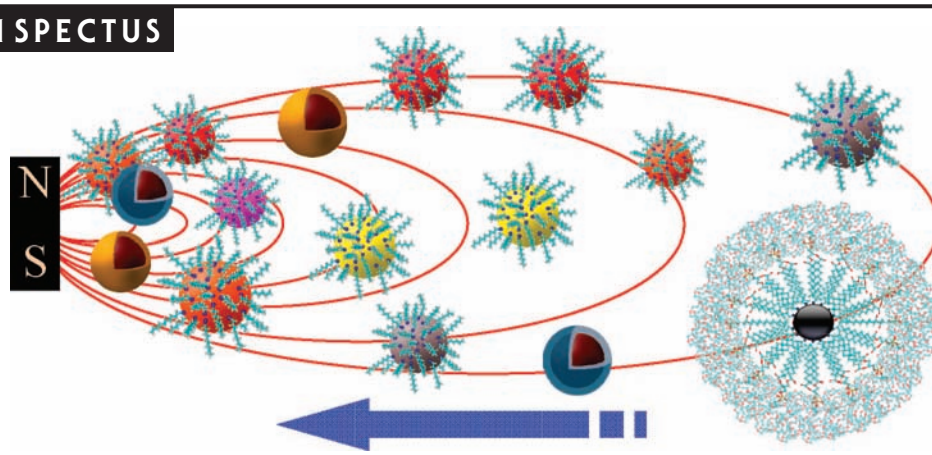

A wide range of metal, magnetic, semiconductor, and polymer nanoparticles with tunable sizes and properties can be synthesized by wet-chemical techniques. Magnetic nanoparticles are particularly attractive because their inherent superparamagnetic properties make them desirable for medical imaging, magnetic field assisted transport, and separations and analyses. With such applications on the horizon, synthetic routes for quickly and reliably rendering magnetic nanoparticle surfaces chemically functional have become an increasingly important focus. This Account describes common synthetic routes for making and functionalizing magnetic nanoparticles and discusses initial applications in magnetic field induced separations.

The most widely studied magnetic nanoparticles are iron oxide (Fe_2O_3 and Fe_3O_4), cobalt ferrite ($CoFe_2O_4$), iron platinum (FePt), and manganese ferrite ($MnFe_2O_4$), although others have been investigated. Magnetic nanoparticles are typically prepared under either high-temperature organic phase or aqueous conditions, producing particles with surfaces that are stabilized by attached surfactants or associated ions. Although it requires more specialized glassware, high-temperature routes are generally preferred when a high degree of stability and low particle size dispersity is desired.

Particles can be further modified with a secondary metal or polymer to create core–shell structures. The outer shells function as protective layers for the inner metal cores and alter the surface chemistry to enable postsynthetic modification of the surfactant chemistry. Efforts by our group as well as others have centered on pathways to yield nanoparticles with surfaces that are both easily functionalized and tunable in terms of the number and variety of attached species. Ligand place-exchange reactions have been shown quite successful for exchanging silanes, acids, thiols, and dopamine ligands onto the surfaces of some magnetic particles. Poly(ethylene oxide)-modified phospholipids can be inserted into nonpolar surface monolayers of as-prepared nanoparticles as a method for modifying the surface chemistry that induces water solubility. In general, reactive termini can subsequently be used to append a range of chemical groups. For example, surfactants with trifluoroethylester or azide termini have been used to attach a range of amine- or alkyne-containing species, respectively.

Chemically functionalized magnetic nanoparticles are promising as advanced materials for analytical separations and analysis. Magnetic field flow fractionation leverages the size-dependent magnetic moments to purify and separate the components of a complex mixture of particles. Similarly, magnetic field gradients are useful for manipulating transport and separation in simple microfluidic devices. By either approach, magnet-induced transport of the particles is a simple method in which an attached reagent, catalyst, or bioanalytical tag can be moved between flow streams within a lab on a chip device.

Published on the Web 02/06/2008 www.pubs.acs.org/acr
10.1021/ar700183b CCC: $40.75

Introduction

The intrinsic interaction of magnetic nanoparticles with applied magnetic field gradients makes these particles attractive for directing transport and separation of attached material that can range in size from molecules to cells.[1] This approach is a powerful way with which to interact with matter at the nanoscale that is complementary to optical methods employing nanoscale noble metal[2,3] and semiconductor particles.[4] As a result, magnetic nanoparticles have garnered widespread attention in recent years to develop and understand synthetic means to control their size, magnetic behavior, and chemical reactivity.[5–8] Simultaneously tuning surface chemistry and physical properties enables preparation of functional magnetic nanoparticles that can be vehicles to manipulate, track, and deliver attached cargo. Varied applications in biomedicine[9–11] and magnetic field assisted separations and analyses[12–16] are envisioned for nanoscale magnets. Extension of the chemistries used to impart surface functionality will give rise to multifunctional magnetic probes and open up new opportunities to perform a wide range of operations using the same particle. Conversely, the size- and composition-dependent magnetic moments[17] hold the potential to be exploited in the development of magnetic-based separation devices. A host of other applications, such as hyperthermia treatment for malignant cells[18] and magnetic resonance imaging (MRI) contrast agents,[19,20] stand to benefit from the unique properties observed in nanoscale magnets.

With recent advancements in synthetic methods has come the ability to easily prepare a wide range of magnetic nanoparticles that are highly crystalline and uniform in size.[21–27] Stabilization of the particles is necessary to induce solubility while preventing agglomeration and, similar to Ag or Au nanoparticles, can be either electrostatic or steric in nature.[28,29] While aqueous methods for magnetic nanoparticles provide electrostatic stabilization of particles, we typically avoid employing these because they often yield particle samples with poor shape and size control and because slight changes in ionic strength or pH can result in precipitation.[30,31] Our interest in bottom-up assembly of nanometer scale materials has led us to adopt high-temperature synthetic methods[21–27] to investigate and explore the characterization, functionalization, and field-assisted transport of magnetic nanoparticles. Applications requiring tunable surface chemistry and magnetism directly benefit from these studies. This Account describes some of the chemistries that we and others have used to make functional nanomagnets and then discusses recent investigations of magnetic field assisted transport of these particles.

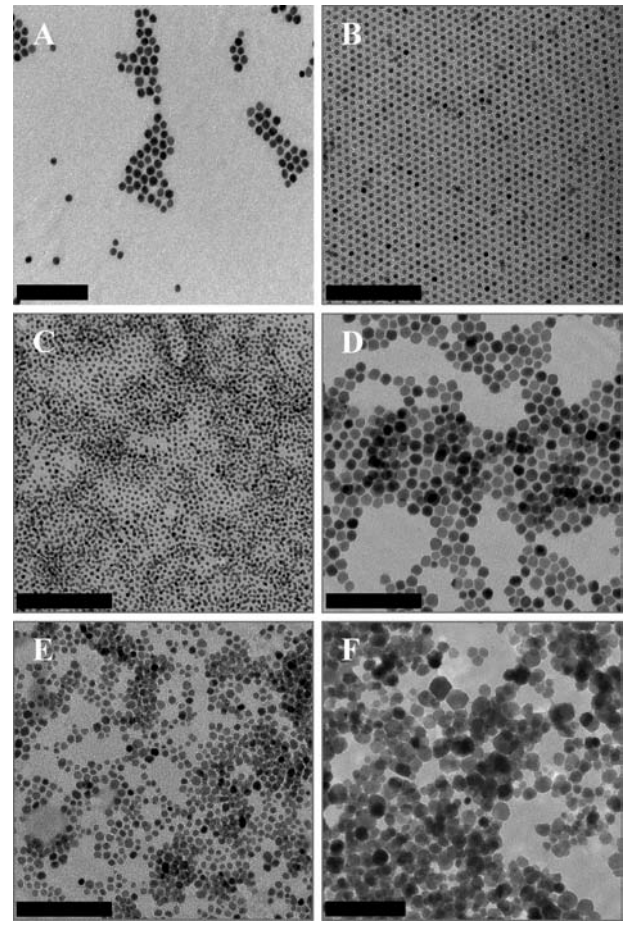

FIGURE 1. TEM images of (A) Au, (B) Fe_2O_3, (C) FePt, (D) $CoFe_2O_4$, (E) $MnFe_2O_4$, and (F) Fe_2O_3(aq) nanoparticles. Scale bars are 100 nm.

Nanoparticle Synthesis

Common high-temperature synthetic methods utilize thermal decomposition[21–27] of metal precursors in the presence of a stabilizing ligand to yield metal nanoparticles ranging in diameter from approximately 3 to 15 nm. The transmission electron microscope (TEM) images in Figure 1 demonstrate the range of sizes and types of materials that are made using the routes shown in Scheme 1. Typical metal precursors include carbonyl[21] and acetylacetonate (acac)[25] complexes (e.g., $Fe(CO)_5$, $Co(acac)_2$, and $Fe(acac)_3$), and the ligands are generally long chain carboxylic acids, amines, or both (e.g., oleic acid and oleylamine). These surfactants are required both to mediate growth during the reaction and to prevent agglomeration of the particles. Shorter chain lengths are sometimes employed to facilitate postsynthetic surface modification,[32] but generally chains with at least six carbons are necessary to provide sufficient stabilization.[24,25,32] Magnetic nanoparticle synthesis and modification is a vigorously studied field that continues to rapidly expand; the key papers described in this

SCHEME 1. Synthesis or Iron Oxide Nanoparticles

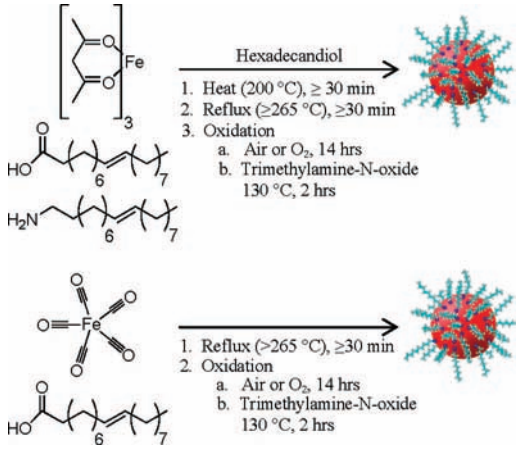

Account are representative of a much larger and growing body of work.

Modifications of the reaction parameters serve as a simple way to tune particle size, shape, and therefore magnetic properties of the nanoparticles. Magnetic moment is intrinsically related to composition: incorporation of Co^{2+} into an iron oxide matrix (i.e., $CoFe_2O_4$) significantly enhances the magnetic anisotropy relative to an iron oxide nanoparticle of equivalent size; conversely, insertion of Mn^{2+} (i.e., $MnFe_2O_4$) decreases the anisotropy.[33] Boiling point (T_b) of the solvent, molar ratio of metal to ligand, and reaction time further affect size and morphology. For example, when $CoFe_2O_4$ particles are synthesized, changing the solvent from phenyl ether ($T_b \approx$ 265 °C, 30 min) to benzyl ether ($T_b \approx$ 298 °C, 2 h) yields a 7 nm increase in size.[25] It has been shown during the synthesis of $MnFe_2O_4$ nanoparticles that a surfactant to Fe ratio smaller than 3:1 yields spherical particles while increasing the ratio to 3:1 results in the synthesis of cubic shapes.[34] These illustrate that exerting control can be accomplished by judicious choice of reaction parameters.

Over the past decade, a wide range of magnetic nanoparticle compositions and structures has been demonstrated, such as the examples shown in the TEM images in Figure 1. The most common of these materials are the iron oxides (Fe_2O_3 and Fe_3O_4), known for their high magnetic moments and biological compatibility, and their corresponding ferrites (e.g., $MnFe_2O_4$ and $CoFe_2O_4$). Metals and alloys such as Mn_3O_4,[35] Fe,[24] Co,[36] Ni,[37] FePt,[22] and FePd[38] are less commonly employed, in part because of their rapid oxidation in air or potential for cytotoxicity. Unlike the more well-known monolayer-protected Au clusters,[2,3] the preparation methods for magnetic nanoparticles do not tolerate the presence of reactive termini on the stabilizing ligands (i.e., -Br, -SH, etc.), either because of thermal instability or because of bonding of the transition metals to the ligands. Therefore the synthesis of magnetic nanoparticles in the presence of functional groups has been largely unsuccessful. As a result, the as-prepared particles often must undergo further modifications and postsynthetic reactions to render them chemically functional.

Core–Shell Particles. An alternate method of particle preparation involves passivation of the magnetic nanoparticles by a secondary metal or polymer. Silica shells have been grown on magnetic nanoparticles to provide a surface that is easily modified with silanes.[39–41] Coating particles with a layer of Au is also highly desirable because of its known reactivity toward sulfur-containing ligands. In both cases, encapsulating particles in an inert shell is thought to provide a protective barrier layer against oxidation or reaction with solution species. Our group demonstrated a facile approach to encapsulate a metal oxide core with Au; γ-Fe_2O_3 nanoparticles prepared by the coprecipitation of Fe salts were used as seeds to nucleate the growth of Au under mildly reducing conditions (scheme in Figure 2A).[42] By addition of sequential aliquots of $HAuCl_4$ and hydroxylamine in the presence of Fe_2O_3 particles, a shell of Au of increasing thickness was deposited on the magnetic particles. This was further evidenced by the growth of a peak in the visible absorption spectrum (Figure 2B) that is associated with the plasmon band for Au. Superconducting quantum interference device (SQUID) magnetometry (Figure 2C) revealed that these particles retained the magnetic properties of the Fe_2O_3. These particles are therefore composite nanomaterials with magnetic cores and a Au surface that enables further chemical functionalization.

Characterization

Magnetic Properties. As ferro- or ferrimagnetic materials decrease in size to the nanometer regime, these change from multidomain to single domain structures, and therefore, superparamagnetic behavior is observed.[43] At room temperature, superparamagnetic materials have no net magnetization and the spins are randomly aligned. These thus act similarly to nonmagnetic nanoparticles. However, exposure to a magnetic field causes the spins in superparamagnetic particles to spontaneously align, magnetizing the particles. When the applied magnetic field is removed, thermal fluctuations result in the complete loss of magnetization. This behavior is highly dependent on temperature, and if the temperature is sufficiently low, thermal fluctuations are not significant enough to randomize the magnetic spins. The temperature at and below which a superparamagnetic particle is permanently magnetized is termed the blocking temperature and is important in the characterization of magnetic nanoparticles. SQUID mag-

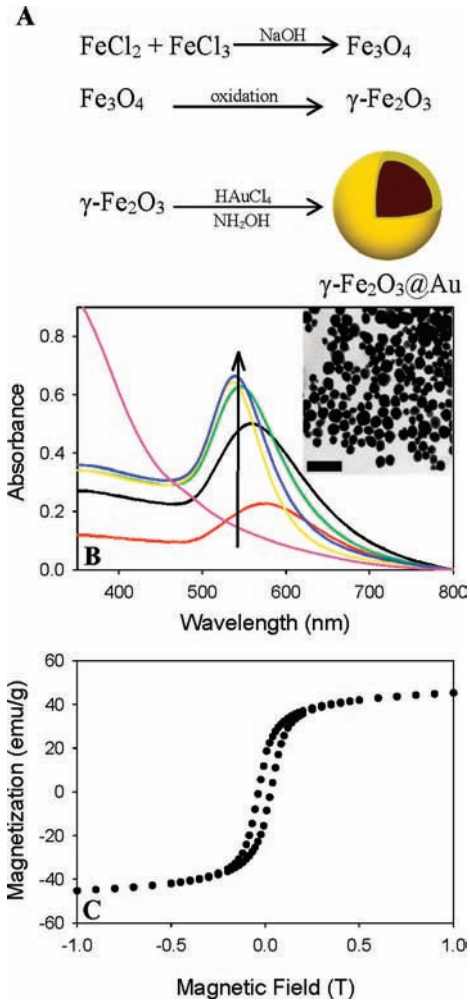

FIGURE 2. (A) Synthetic scheme for synthesis of γ-Fe_2O_3/Au core/shell nanoparticles. (B) UV–vis spectra of as-synthesized γ-Fe_2O_3 (purple) particles, and following iterative Au additions one (red), two (black), three (green), four (yellow), and five (blue). The inset shows a TEM image of the γ-Fe_2O_3/Au core/shell nanoparticles after five iterative additions. Scale bar is 200 nm. (C) Magnetization at 5 K as a function of applied field for γ-Fe_2O_3/Au core/shell nanoparticles.

netometry is routinely used to assess these magnetic properties. Monitoring magnetization as a function of temperature for particles cooled with and without an applied magnetic field followed by warming in the presence of a magnetic field allows the characteristic blocking temperature to be determined.

Core Size and Composition. Uniformity in size and shape is highly desirable in nanoparticle synthesis since physical properties strongly depend on both of these. Unlike noble metal and semiconductor nanoparticles, magnetic particles possess neither fluorescence nor surface plasmon absorption to assist in characterization of particle size. Therefore, the most common characterization method for magnetic nanoparticles is TEM. Low-resolution TEM is used to measure core size and size uniformity (i.e., monodispersity) and is typically accompanied with energy-dispersive X-ray spectroscopy (EDX) to provide elemental analysis. High-resolution TEM can provide electron diffraction from a single nanoparticle and atomic resolution of the crystal lattice. In some cases, scanning TEM (STEM) methods coupled with electron-energy loss spectroscopy (EELS) yield elemental analysis at subnanometer lateral resolution.

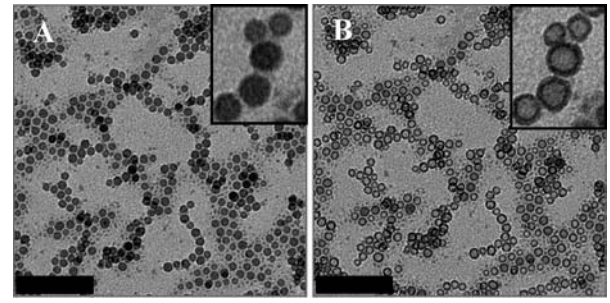

FIGURE 3. TEM images of amorphous iron oxide nanoparticles synthesized with hexadecylamine/trioctylphosphine oxide (A) before and (B) after 2 min of electron beam irradiation. Scale bars are 100 nm.

Recently, while investigating the structure of nanoparticles using TEM, our laboratory observed that electron beam irradiation can result in significant changes to particle morphology.[44] Amorphous iron oxide nanoparticles synthesized using a mixture of hexadecylamine and trioctlyphosphine oxide initially appeared to be solid; however, less than 2 min of electron beam irradiation resulted in the morphological changes shown in Figure 3. Formation of hollow particles was attributed to electron beam induced structural rearrangements, which suggested that TEM analysis of nanoparticle structure can cause changes in particles that can easily lead to misinterpretation of the as-prepared structures. Since the original paper, our continuing studies of TEM-induced transformation have shown that this effect appears to be more general and occurs in additional amorphous systems (i.e., varied ligands and metal oxides). These data imply that time-resolved TEM analysis is ultimately necessary to rule out structural transformations caused by the microscope versus particles that form hollow shells via the Kirkendall effect.[45,46]

Functionalization

Development of methods aimed at the postsynthetic surface modification of magnetic nanoparticles is important to render them chemically functional and to control their solubility. For biomedical applications and bioanalysis, the ability to solubilize the nanoparticles in water and to modify their surfaces with molecules, proteins, oligonucleotides, or other targeting agents, is a crucial step toward their widespread use. Conversely, materials applications of magnetic particles will

SCHEME 2. Selected Functionalization Routes for Magnetic Nanoparticles

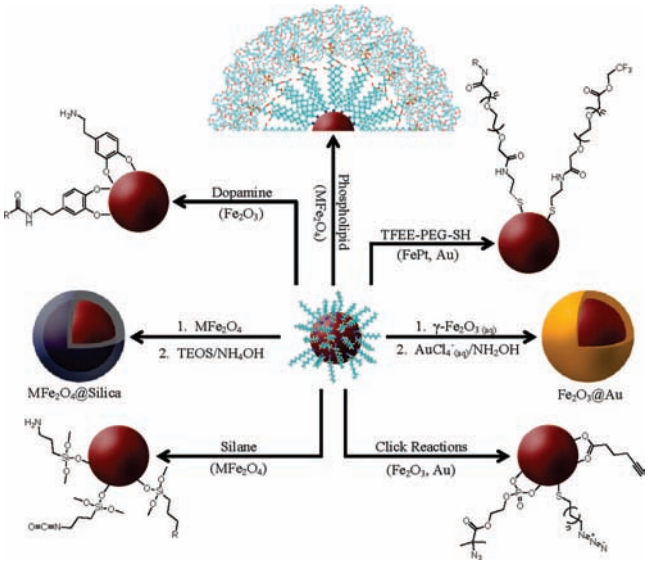

likely require a broad range of chemical functionalization and solvent compatibility. We have therefore sought synthetic routes by which these may be achieved; these are generally outlined and contrasted to other available methods in Scheme 2.

Ligand Place Exchange. Place-exchange reactions on the surface of Au nanoparticles were pioneered by Murray et al. and provide a way to append chemically functional species.[3] To an extent, these reactions should be applicable to magnetic nanoparticles, but differences in metal and metal oxide affinity for ligands is a key factor in the efficacy of place exchange. One of the first demonstrations of using place exchange was on FePt magnetic particles, which were stirred in a solution containing thiol-modified nitrilotriacetic (NTA) acid. Metal−sulfur bonds replaced the hydrophobic surface monolayer and resulted in water-soluble and functional particles.[47] Attachment of poly(ethylene glycol) (PEG) to FePt nanoparticles was later demonstrated via ligand exchange, rendering the FePt particles water-soluble.[32] Similarly, place exchange of dopamine onto Fe_2O_3 nanoparticles[32,48−50] has also been utilized to prepare water-soluble magnetic particles. The broad applicability of this latter approach is not yet known, but attachment schemes for molecules other than dopamine and incorporating tags for postsynthetic modification are clearly needed.

To address this need for facile and broadly applicable methods to impart tunable functionality to magnetic particles, our laboratory recently synthesized a trifluoroethylester (TFEE)-terminated PEG−thiol shown in Scheme 3A. This ligand was designed such that the PEG confers water solubility, the thiol

SCHEME 3. General Routes for Use of TFEE−PEG−SH for the Functionalization of Nanoparticles[a]

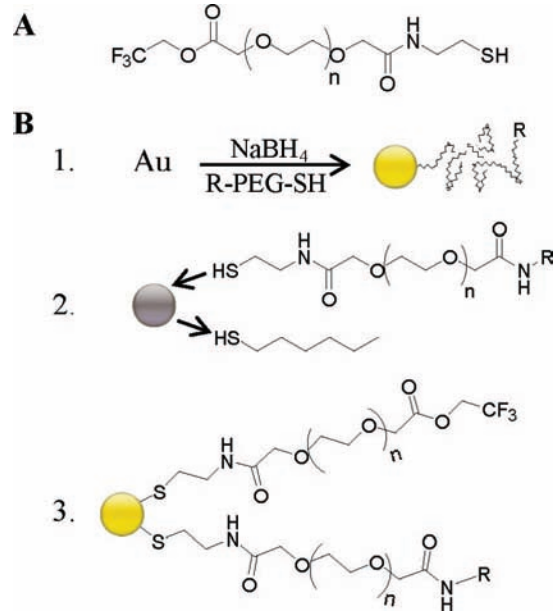

[a] (A) TFEE−PEG−SH molecule; (B1) direct synthesis in the presence of a modified R−PEG−SH ligand (shown as a random coil; R = functionality added via amide linkage); (B2) ligand place exchange of R−PEG−SH onto existing nanoparticles (Au or magnetic FePt); (B3) exchange of TFEE−PEG−SH onto Au nanoparticles followed by subsequent reaction.

terminus provides an anchor to attach to metal particle surfaces, and the TFEE terminus reacts with primary amines at room temperature to form amide bonds without the need for coupling reagents. This ligand was attached to FePt and Au nanoparticles using the methods shown in Scheme 3B.[51] The resulting particles were solubilized in aqueous solutions and could be reacted with a range of primary amine-containing molecules, including fluorescamine, biotin, pyridine, and aliphatic reactants. Biotinylation rendered the particles compatible with existing bioconjugation methods. Conversely, the TFEE ligand was reacted with diethylamine to produce amine termini and then attached to FePt nanoparticles. A titration of these amine-terminated FePt nanoparticles with fluorescamine is shown in Figure 4; the emission spectra show that the product particles are fluorescent, in addition to being water-soluble. This route thus provides attractive agents for both fluorescence-based detection and magnetic separation of biological species.

Silanes bind to ferrite nanoparticles (MFe_2O_4, M = Fe, Co, Mn) and can also be place-exchanged onto particles as an alternate method of tuning surface chemistry and solubility.[19,20,52] For example, attachment of silane monolayers containing amino, aldehyde, thiol, cyano, and isocyanate has been demonstrated.[20] Silane-modified Fe_2O_3 nanoparticles have been used *in vivo* as MRI contrast agents and as a detection scheme for monitoring glioma cells.[19,20]

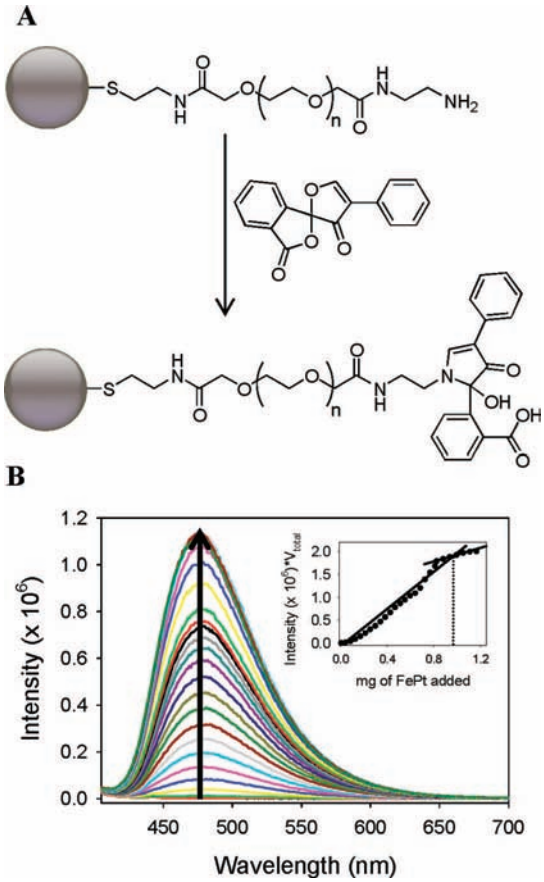

FIGURE 4. (A) Reaction of $H_2NC_2H_4NH-PEG-SH$-substituted FePt nanoparticles with fluorescamine and (B) fluorescence emission spectra of a dichloromethane solution containing 0.02 μmol of fluorescamine during the sequential addition of 20 μL aliquots of $H_2NC_2H_4NH-PEG-SH$-modified FePt particles (1.42 mg/mL). Excitation wavelength is 390 nm. The inset shows emission intensity at 475 nm vs quantity of added FePt particles.

Click Chemistry. A new functionalization route that holds great promise as a general method for materials applications is the use of "click" chemistry, which was initially reported for nanoparticles by our laboratory[53] and further studied by others.[54] Although click chemistry refers to a class of reactions, herein we refer to 1,3-dipolar cycloadditions that occur by combination of azide-containing species with ethynyl groups to form a 1,2,3-triazole ring as in Scheme 4.[55] Although this has been widely used in organic chemistry and for the modification of Au electrode surfaces,[56] our group was the first to apply it to the modification of Au nanoparticles by reacting azide-terminated ligands with alkyne-containing species at room temperature in uncatalyzed reactions. The general utility of this approach lies in the ability to react any alkyne-containing molecule, which was demonstrated with species including ferrocene, pyrene, and PEG.

The Turro group further elaborated on this method to functionalize Fe_2O_3 nanoparticles; alkyne-containing organophosphates and carboxylates were exchanged onto the surface of oleic acid stabilized Fe_2O_3 nanoparticles.[54] Cu-catalyzed triazole formation was used to append alkyl halide, benzene, and polymeric (α-acetylene−poly(*tert*-butyl acrylate)) species. Taken together, these papers[53,54] point toward a potentially broad adaptability of click chemistry for nanoparticle functionalization.

Micelle Encapsulation. One of the most versatile routes developed for quantum dot modification,[57] which was subsequently adapted to magnetic nanoparticles by our group[58,13] and others,[59] is the encapsulation of hydrophobic nanoparticles within phospholipid micelles. To accomplish this, modified lipids containing attached poly(ethylene glycol) chains are added to solutions of nanoparticles passivated with a monolayer of alkyl chains (e.g., oleic acid). Lipid chains intercalate into the nanoparticle monolayer because of favorable partitioning and intermolecular forces, which results in a micelle-like structure with the PEG termini forming a hydrophilic shell as depicted in Scheme 2. It has recently been shown that charge-neutral amphiphilic polymers[60] and fatty alcohols[61] could similarly be used to encapsulate nanoparticles.

The ω-terminal end of the PEG−phospholipid chain can contain a range of chemical functionalities including biotin, acid, amine, maleimide, and folic acid groups. The extent of particle functionalization is determined by controlling the relative amounts of ω-substituted versus methyl-terminated lipids. The assumption is generally made that this solution ratio is translated to the relative percentage surrounding the nanoparticle, although it remains an analytical challenge to confirm this without digestion of the particles. Our laboratory has demonstrated that phospholipid encapsulation is generally useful for magnetic nanoparticles synthesized with a hydrophobic monolayer, including Fe_2O_3,[13] $MnFe_2O_4$,[13] and $CoFe_2O_4$[58,62] nanoparticles. We have therefore used phospholipids to prepare water-soluble and functional magnetic nanoparticles for use in microfluidics[13] and for attachment to motor proteins to control patterning and transport.[58,62]

Magnetic Field Assisted Transport

Application of an external magnetic field gradient to a magnetic nanoparticle causes magnetization and subsequent movement due to the force acting on it as defined by[15,16]

$$F_m = \frac{V\Delta\chi}{\mu_0}(B \cdot \nabla)B \qquad (1)$$

where V is the volume of the particle, $\Delta\chi$ is the difference in magnetic susceptibilities of the particle and solvent, μ_0 is the vacuum permeability, B is the magnetic field strength and ∇

SCHEME 4. Click Functionalization of (A) Au and (B) Fe_2O_3 nanoparticle surfaces[a]

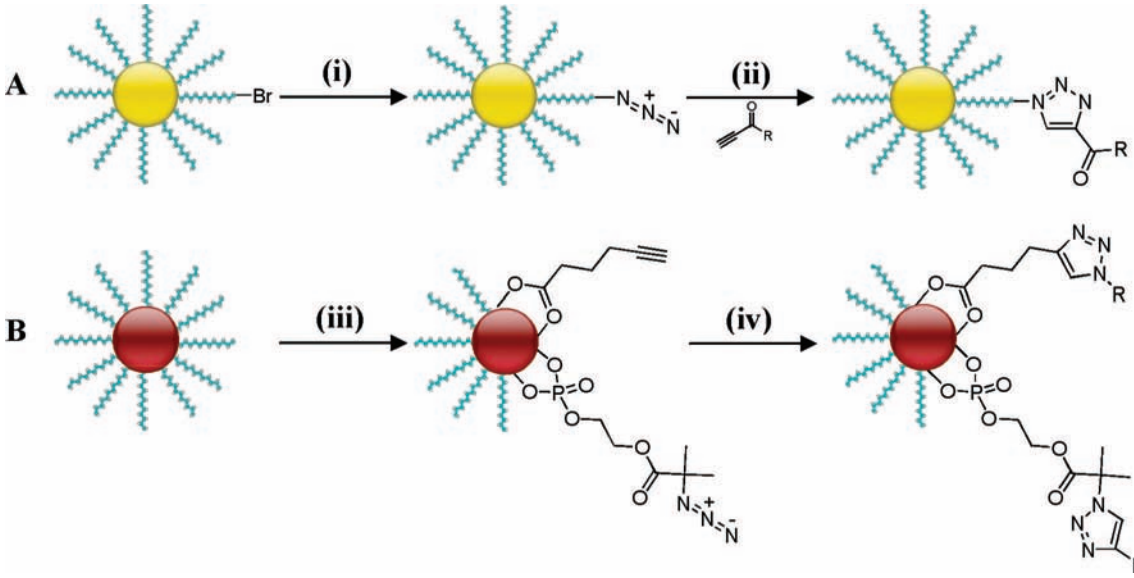

[a] Conditions for reaction A: (i) 0.25 M NaN_3 in DCM/DMSO solution, 48 h; (ii) R = propyn-1-one derivatized compound in dioxane or 1:1 hexane/dioxane.[53] Conditions for reaction B: (iii) exchange of either phosphonic acid or hexynoic acid ligands; (iv) DMSO/H_2O, $CuSO_4 \cdot 5H_2O$, 24 h.[54]

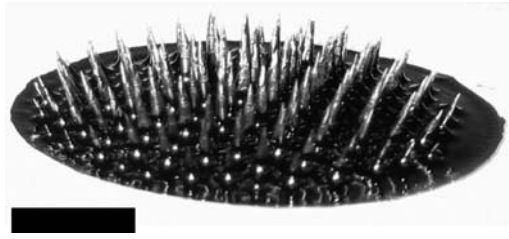

FIGURE 5. Photograph of a concentrated solution of $CoFe_2O_4$ nanoparticles in hexane placed on top of a permanent magnet (~0.4 T). Scale bar is 1 cm.

FIGURE 6. Diagram of magnetic particle separation in capillary MFFF. Weakly interacting particles have a larger average layer thickness (h_A) and elute at shorter times; strong interaction results in the smallest layer thickness (h_C).

is the field gradient. In the absence of a field gradient, the net force acting on the particle is zero. However with a gradient, an applied force (F_m) acts on the particles and results in movement toward the highest field strength. Surfactant monolayers prevent irreversible aggregation and precipitation when the field is applied. For very concentrated solutions of magnetic nanoparticles (i.e., >100 mg/mL) called ferrofluids, the attraction to the magnetic field gives rise to the well-known Rosensweig effect[63] (Figure 5), in which the entire solution of magnetic particles (including the solvent) conforms to the magnetic field lines. Applications of ferrofluids include cooling systems for loudspeakers and bearings for frictionless sealing.[1]

Magnetic Field Flow Fractionation. Magnetic nanomaterials will ultimately be able to perform specific chemical tasks dictated by their attached groups and be manipulated with a magnetic gradient to an extent governed by the particles' magnetic properties. While we have briefly described our efforts toward chemical functionalization, to investigate magnetic field manipulation of particles, our group turned to magnetic field flow fractionation (MFFF), which separates species on the basis of their magnetic susceptibility and is applicable to material with sizes from nanometers to micrometers.[64] Shown schematically in Figure 6, MFFF causes sample injected into a capillary to interact with an external magnetic field gradient that forces it toward the accumulation wall (i.e., higher field strength). Material that interacts strongly with the field is restricted to the slower flow streams near the walls of the channel, while material that interacts weakly is free to experience the faster flow streams toward the center of the channel.

Our group was the first to demonstrate successful implementation of MFFF to separate and purify magnetic nanoparticle samples.[12] Although theoretically the ideal channel geometry is rectangular,[65] the use of flexible fused silica capillary in our experiments allowed the use of a NdFeB permanent magnet and a simple system using standard laboratory components. This magnet had a relatively strong magnetic field (~0.3 T) applied roughly orthogonal to the flow within the capillary. This simple benchtop instrument demonstrated the retention of nanoparticle samples as a

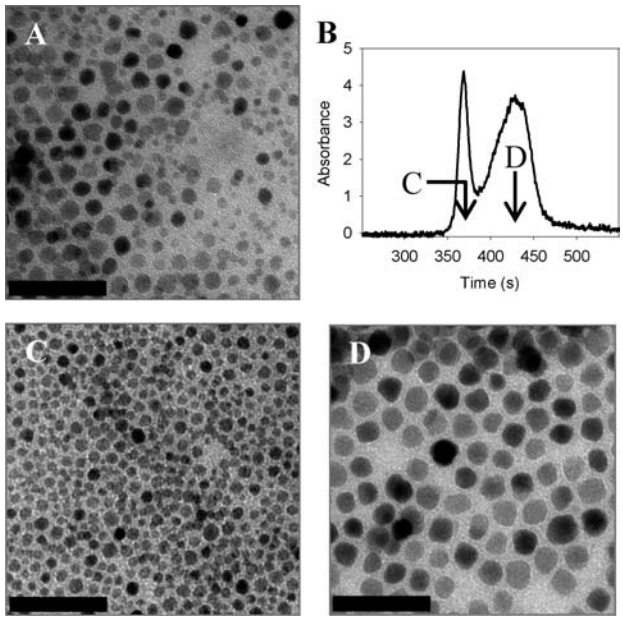

FIGURE 7. (A) TEM image of a mixture of 6 nm Fe_2O_3 and 13 nm $CoFe_2O_4$ nanoparticles and (B) MFFF of a 1.3 μL injection of a hexane solution of this mixture in the presence of the magnet, with arrows indicating times when the samples shown in the TEM images in panels C and D were collected. Scale bars are 50 nm.

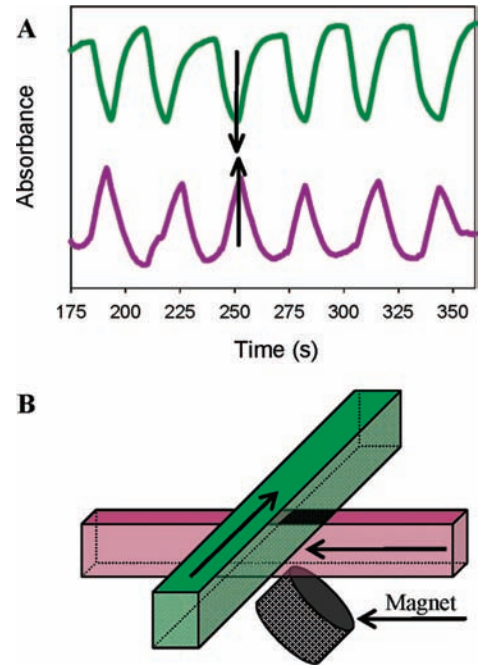

FIGURE 8. (A) Absorbance versus time for both the upper (green) and lower (purple) channels while varying the magnet placement (~10 s on/~20 s off) with a continuous stream of Fe_2O_3 nanoparticles flowing through the upper channel at 15 μL/min and (B) diagram of the crossed channels (arrows indicate direction of pressure-driven flow) with a NdFeB permanent magnet placed beneath the channel intersection. Green and purple designate upper and lower channels, respectively.

function of the solvent flow rate and nanoparticle size and composition. In Figure 7, a mixture of Au and Fe_2O_3 nanoparticles was separated into size-monodisperse fractions using MFFF. Ongoing improvements to this method and the inclusion of a tunable magnetic field strength will ultimately allow for the simple purification of highly multiplexed functionalized magnetic nanoparticle mixtures for biological analysis and detection.

Applications to Microfludics. Controlling the placement and movement of nanoparticles within microchannels via an external magnetic field precludes the need for microfabricated components, is compatible with existing magnetic bead bioassays, and provides a tempting alternative to standard methods of analyte control and injection. Our group recently studied the ability to move, manipulate, and inject magnetic nanoparticles within the simple crossed-channel microfluidic device shown schematically in Figure 8B.[13] The transit of particles through the channels is monitored using an absorption detector, which confirms the presence of nanoparticles in a flow stream. A permanent magnet placed beneath the channel intersection selectively redirected magnetic nanoparticles from one channel to the other but did not affect the motion of nonmagnetic Au nanoparticles. In Figure 8A, when the magnet position was varied, the magnetic nanoparticle solution was periodically pulled into the lower flow stream, which was monitored by the change in absorbance. Thus, this is a simple method to control the injection of nanoparticle reactants in a microchannel. For future applications, this demonstrates the ability to use weak and inexpensive magnets to inject and manipulate molecules, catalysts, or reagents that are bound to the magnetic particle surface.

Conclusions

In this Account, we have described contributions from our laboratory and others toward the advancement of characterization, functionalization, and use of magnetic nanoparticles to control transport. Exploiting the tunable surfaces of these materials holds promise for creating single nanoparticle vehicles capable of analyte targeting and delivery, while the intrinsic magnetic properties of the particles enable directed transport and diagnostic imaging. With interest in microfluidic devices capable of performing highly multiplexed analytical tasks, development of magnetically controlled transport of these particles will ultimately provide a unique way to manipulate mixing, switching, and analyte capture. For example, we envision that the selective separation of particles based on their size-dependent magnetic moments will be leveraged to bind and purify complex mixtures into individual components. Further

expansion of magnetic nanoparticles as analytical tools will require continued expansion of the library of functional nanoparticle surface chemistries and will build on these methods for magnetic manipulation.

We are grateful for the students and research associates who have contributed to the above studies including D. Fleming, B. Hutchins, J. Lyon, M. Platt, and C. J. Thode, as well as our collaborators W. Hancock (PSU Bioengineering) and R. Freitas, M. Wilson, M. Stone, and P. Schiffer (PSU Physics). This work is generously supported by the National Science Foundation (Grant CHE0239-702), the American Chemical Society Petroleum Research Fund (Grant ACS PRF 37553-G4), the Penn State Center for Nanoscale Science (Grant MRSEC DMR0213623), and a 3M nontenured faculty grant. A.H.L gratefully acknowledges support from an ACS Division of Analytical Chemistry Graduate Research Fellowship (sponsored by Eli Lilly & Company) and from the Lubrizol Foundation.

BIOGRAPHICAL INFORMATION

Andrew H. Latham is a graduate of Salem State College in Salem, Massachusetts (B.S., 2003). He is currently a fifth-year graduate student in the Ph.D. program at PSU working in Professor Williams' laboratory.

Mary Elizabeth Williams is an Associate Professor in the Department of Chemistry at Penn State whose active research group is broadly interested in bottom-up assembly of nanostructured inorganic materials for analysis and separation, electronics, and photoinduced electron transfer.

FOOTNOTES

*Corresponding author. Phone: (814) 865-8859. Fax: (814) 865-3292. E-mail: mbw@chem.psu.edu.

REFERENCES

1 Odenbach, S. Magnetic Fluids - Suspensions of Magnetic Dipoles and Their Magnetic Control. *J. Phys.: Condens. Matter* **2003**, *15*, S1497–S1508.

2 Daniel, M.-C.; Astruc, D. Gold Nanoparticles: Assembly, Supramolecular Chemistry, Quantum Size-Related Properties, and Applications toward Biology, Catalysis, and Nanotechnology. *Chem. Rev.* **2004**, *104*, 293–346.

3 Templeton, A. C.; Wuelfing, W. P.; Murray, R. W. Monolayer-Protected Cluster Molecules. *Acc. Chem. Res.* **2000**, *33*, 27–36.

4 Michalet, X.; Pinaud, F.; Lacoste, T. D.; Maxime, D.; Bruchez, M. P.; Alivisatos, A. P.; Weiss, S. Properties of Fluorescent Semiconductor Nanocrystals and their Application to Biological Labeling. *Single Mol.* **2001**, *4*, 261–276.

5 Hyeon, T. Chemical Synthesis of Magnetic Nanoparticles. *Chem. Commun.* **2003**, 927–934.

6 Huber, D. L. Synthesis, Properties, and Applications or Iron Nanoparticles. *Small* **2005**, *1*, 482–501.

7 Cushing, B. L.; Kolesnichenko, V. L.; O'Connor, C. J. Recent Advances in the Liquid-Phase Syntheses of Inorganic Nanoparticles. *Chem. Rev.* **2004**, *104*, 3893–3946.

8 Murray, C. B.; Kagan, C. R.; Bawendi, M. G. Synthesis and Characterization of Monodisperse Nanocrystals and Close-Packed Nanocrystal Assemblies. *Annu. Rev. Mater. Sci.* **2000**, *30*, 545–610.

9 Pankhurst, Q. A.; Connolly, J.; Jones, S. K.; Dobson, J. Applications of Magnetic Nanoparticles in Biomedicine. *J. Phys. D: Appl. Phys.* **2003**, *36*, R167–R181.

10 Tartaj, P.; Morales, M. P.; Veintemillas-Verdaguer, S.; González-Carreño, T.; Serna, C. J. The Preparation of Magnetic Nanoparticles for Applications in Biomedicine. *J. Phys. D: Appl. Phys.* **2003**, *36*, R182–R197.

11 Berry, C. C.; Curtis, A. S. G. Functionalisation of Magnetic Nanoparticles for Applications in Biomedicine. *J. Phys. D: Appl. Phys.* **2003**, *36*, R198–R206.

12 Latham, A. H.; Freitas, R. S.; Schiffer, P.; Williams, M. E. Capillary Magnetic Field Flow Fractionation and Analysis of Magnetic Nanoparticles. *Anal. Chem.* **2005**, *77*, 5055–5062.

13 Latham, A. H.; Tarpara, A. N.; Williams, M. E. Magnetic Field Switching of Nanoparticles between Orthogonal Microfluidic Channels. *Anal. Chem.* **2007**, *79*, 5746–5752.

14 Pamme, N.; Manz, A. On-Chip Free-Flow Magnetophoresis: Continuous Flow Separation of Magnetic Particles and Agglomerates. *Anal. Chem.* **2004**, *76*, 7250–7256.

15 Pamme, N. Magnetism and Microfluidics. *Lab Chip* **2006**, *6*, 24–38.

16 Gijs, M. A. M. Magnetic Bead Handling On-Chip: New Opportunities for Analytical Applications. *Microfluid. Nanofluid.* **2004**, *1*, 22–40.

17 Roca, A. G.; Morales, M. P.; O'Grady, K.; Serna, C. J. Structural and Magnetic Properties of Uniform Magnetite Nanoparticles Prepared by High Temperature Decomposition of Organic Precurors. *Nanotechnology* **2006**, *17*, 2783–2788.

18 Chan, D. C. F.; Kirpotin, D. B.; Bunn, P. A. Synthesis and Evaluation of Colloidal Magnetic Iron Oxides for the Site-Specific Radiofrequency-Induced Hyperthermia of Cancer. *J. Magn. Magn. Mater.* **1993**, *122*, 374–378.

19 Veiseh, O.; Sun, C.; Gunn, J.; Kohler, N.; Gabikian, P.; Lee, D.; Bhattarai, N.; Ellenbogen, R.; Sze, R.; Hallahan, A.; Olson, J.; Zhang, M. Optical and MRI Multifunctional Nanoprobe for Targeting Gliomas. *Nano Lett.* **2005**, *5*, 1003–1008.

20 Huh, Y.-M.; Jun, Y.-W.; Song, H.-T.; Kim, S.; Choi, J.-S.; Lee, J.-H.; Yoon, S.; Kim, K.-S.; Shin, J.-S.; Suh, J.-S.; Cheon, J. In Vivo Magnetic Resonance Detection of Cancer by Using Multifunctional Magnetic Nanocrystals. *J. Am. Chem. Soc.* **2005**, *127*, 12387–12391.

21 Woo, K.; Hong, J.; Choi, S.; Lee, H.-W.; Ahn, J.-P.; Kim, C. S.; Lee, S. W. Easy Synthesis and Magnetic Properties of Iron Oxide Nanoparticles. *Chem. Mater.* **2004**, *16*, 2814–2818.

22 Sun, S.; Murray, C. B.; Weller, D.; Folks, L.; Moser, A. Mondisperse FePt Nanoparticles and Ferromagnetic FePt Nanocrystal Superlattices. *Science* **2000**, *287*, 1989–1992.

23 Sun, S.; Zeng, H. Size-Controlled Synthesis of Magnetite Nanoparticles. *J. Am. Chem. Soc.* **2002**, *124*, 8204–8205.

24 Hyeon, T.; Lee, S. S.; Park, J.; Chung, Y.; Na, H. B. Synthesis of Highly Crystalline and Monodisperse Maghemite Nanocrystallites without a Size-Selection Process. *J. Am. Chem. Soc.* **2001**, *123*, 12798–12801.

25 Sun, S.; Zeng, H.; Robinson, D. B.; Raoux, S.; Rice, P. M.; Wang, S. X.; Li, G. Monodisperse MFe_2O_4 (M = Fe, Co, Mn) Nanoparticles. *J. Am. Chem. Soc.* **2004**, *126*, 273–279.

26 Park, J.; An, K.; Hwang, Y.; Park, J.-G.; Noh, H.-J.; Kim, J.-Y.; Park, J.-H.; Hwang, N.-M.; Hyeon, T. Ultra-Large-Scale Syntheses of Monodisperse Nanocrystals. *Nat. Mater.* **2004**, *3*, 891–895.

27 Hyeon, T.; Chung, Y.; Park, J.; Lee, S. S.; Kim, Y.-W.; Park, B.-H. Synthesis of Highly Crystalline and Monodisperse Cobalt Ferrite Nanocrystals. *J. Phys. Chem. B* **2002**, *106*, 6831–6833.

28 Frens, G. Controlled Nucleation for the Regulation of the Particle Size in Monodisperse Gold Suspensions. *Nature* **1973**, *241*, 20–22.

29 Brust, M.; Walker, M.; Bethell, D.; Schiffrin, D. J.; Whyman, R. Synthesis of thiol-derivatized gold nanoparticles in a two-phase liquid-liquid system. *J. Chem. Soc., Chem. Commun.* **1994**, 801–802.

30 Neveu, S.; Bee, A.; Robineau, M.; Talbot, D. Size-Selective Chemical Synthesis of Tartrate Stabilized Cobalt Ferrite Ionic Magnetic Fluid. *J. Colloid Interface Sci.* **2002**, *255*, 293–298.

31 Kang, Y. S.; Risbud, S.; Rabolt, J. F.; Stroeve, P. Synthesis and Characterization of Nanometer-Size Fe_3O_4 and γ-Fe_2O_3 Particles. *Chem. Mater.* **1996**, *8*, 2209–2211.

32 Hong, R.; Fischer, N. O.; Emrick, T.; Rotello, V. M. Surface PEGylation and Ligand Exchange Chemistry of FePt Nanoparticles for Biological Applications. *Chem. Mater.* **2005**, *17*, 4617–4621.

33 West, A. R. *Basic Solid State Chemistry*; John Wiley & Sons: New York, 1988; pp 356–359.

34 Zeng, H.; Rice, P. M.; Wang, S. X.; Sun, S. Shape-Controlled Synthesis and Shape-Induced Texture of $MnFe_2O_4$ Nanoparticles. *J. Am. Chem. Soc.* **2004**, *126*, 11458–11459.

35 Seo, W. S.; Jo, H. H.; Lee, K.; Kim, B.; Oh, S. J.; Park, J. T. Size-Dependent Magnetic Properties of Colloidal Mn_3O_4 and MnO Nanoparticles. *Angew. Chem., Int. Ed.* **2004**, *43*, 1115–1117.

36 Sun, S.; Murray, C. B. Synthesis of Monodisperse Cobalt Nanocrystals and Their Assembly into Magnetic Superlattices. *J. Appl. Phys.* **1999**, *85*, 4325–4330.

37 Park, J.; Kang, E.; Son, S. U.; Park, H. M.; Lee, M. K.; Kim, J.; Kim, K. W.; Noh, H.-J.; Park, J.-H.; Bae, C. J.; Park, J.-G.; Hyeon, T. Monodisperse Nanoparticles of

Ni and NiO: Synthesis, Characterization, Self-Assembled Superlattices, and Catalytic Applications in the Suzuki Coupling Reaction. *Adv. Mater.* **2005**, *17*, 429–434.

38 Chen, M.; Nikles, D. E. Synthesis of Spherical FePd and CoPt Nanoparticles. *J. Appl. Phys.* **2002**, *91*, 8477–8479.

39 Lu, C.-W.; Hung, Y.; Hsiao, J.-K.; Yao, M.; Chung, T.-H.; Lin, Y.-S.; Wu, S.-H.; Hsu, S.-C.; Liu, H.-M.; Mou, C.-Y.; Yang, C.-S.; Huang, D.-M.; Chen, Y.-C. Bifunctional Magnetic Silica Nanoparticles for Highly Efficient Human Stem Cell Labeling. *Nano Lett.* **2007**, *7*, 149–154.

40 Bonini, M.; Wiedenmann, A.; Baglioni, P. Synthesis and Characterization of Surfactant and Silica-Coated Cobalt Ferrite Nanoparticles. *Physica A* **2004**, *399*, 86–91.

41 Wagner, J.; Autenrieth, T.; Hempelmann, R. Core Shell Particles Consisting of Cobalt Ferrite and Silica as Model Ferrofluids [$CoFe_2O_4$-SiO_2 Core Shell Particles]. *J. Magn. Magn. Mater.* **2002**, *252*, 4–6.

42 Lyon, J. L.; Fleming, D. A.; Stone, M. B.; Schiffer, P.; Williams, M. E. Synthesis of Fe Oxide Core/Au Shell Nanoparticles by Iterative Hydroxylamine Seeding. *Nano Lett.* **2004**, *4*, 719–723.

43 Bean, C. P.; Livingston, J. D. Superparamagnetism. *J. Appl. Phys.* **1959**, *30*, 120S–129S.

44 Latham, A. H.; Wilson, M. J.; Schiffer, P.; Williams, M. E. TEM-Induced Structural Evolution in Amorphous Fe Oxide Nanoparticles. *J. Am. Chem. Soc.* **2006**, *128*, 12632–12633.

45 Yin, Y.; Rioux, R. M.; Erdonmez, C. K.; Hughes, S.; Somorjai, G. A.; Alivisatos, A. P. Formation of Hollow Nanocrystals through the Nanoscale Kirkendall Effect. *Science* **2004**, *304*, 711–714.

46 Chiang, R.-K.; Chiang, R.-T. Formation of Hollow Ni_2P Nanoparticles Based on the Nanoscale Kirkendall Effect. *Inorg. Chem.* **2007**, *46*, 369–371.

47 Xu, C.; Xu, K.; Gu, H.; Zhong, X.; Guo, Z.; Zheng, R.; Zhang, X.; Xu, B. Nitrilotriacetic Acid-Modified Magnetic Nanoparticles as a General Agent To Bind Histidine-Tagged Proteins. *J. Am. Chem. Soc.* **2004**, *126*, 3392–3393.

48 Xu, C.; Xu, K.; Gu, H.; Zheng, R.; Liu, H.; Zhang, X.; Guo, Z.; Xu, B. Dopamine as a Robust Anchor To Immobilize Functional Molecules on the Iron Oxide Shell of Magnetic Nanoparticles. *J. Am. Chem. Soc.* **2004**, *126*, 9938–9939.

49 Bagaria, H. G.; Ada, E. T.; Shamsuzzoha, M.; Nikles, D. E.; Johnson, D. T. Understanding Mercapto Ligand Exchange on the Surface of FePt Nanoparticles. *Langmuir* **2006**, *22*, 7732–7737.

50 Shultz, M. D.; Reveles, J. U.; Khanna, S. N.; Carpenter, E. E. Reactive Nature of Dopamine as a Surface Functionalization Agent in Iron Oxide Nanoparticles. *J. Am. Chem. Soc.* **2007**, *129*, 2482–2487.

51 Latham, A. H.; Williams, M. E. Versatile Routes toward Functional, Water-Soluble Nanoparticles via Trifluoroethylester-PEG-Thiol Ligands. *Langmuir* **2006**, *22*, 4319–4326.

52 Palma, R. D.; Peeters, S.; Van Bael, M. J.; Van den Rul, H. V.; Bonroy, K.; Laureyn, W.; Mullens, J.; Borghs, G.; Maes, G. Silane Ligand Exchange to Make Hydrophobic Superparamagnetic Nanoparticles Water-Dispersible. *Chem. Mater.* **2007**, *19*, 1821–1831.

53 Fleming, D. A.; Thode, C. J.; Williams, M. E. Triazole Cycloaddition as a General Route for Functionalization of Au Nanoparticles. *Chem. Mater.* **2006**, *18*, 2327–2334.

54 White, M. A.; Johnson, J. A.; Koberstein, J. T.; Turro, N. J. Toward the Syntheses of Universal Ligands for Metal Oxide Surfaces: Controlling Surface Functionality through Click Chemistry. *J. Am. Chem. Soc.* **2006**, *128*, 11356–11357.

55 Huisgen, R. Kinetics and Reaction Mechanisms: Selected Examples from the Experience of Forty Years. *Pure Appl. Chem.* **1989**, *61*, 613–628.

56 Collman, J. P.; Devaraj, N. K.; Eberspacher, T. P. A.; Chidsey, C. E. D. Mixed Azide-Terminated Monolayers: A Platform for Modifying Electrode Surfaces. *Langmuir* **2006**, *22*, 2457–2464.

57 Dubertret, B.; Skourides, P.; Norris, D. J.; Noireaux, V.; Brivanlou, A. H.; Libchaber, A. In Vivo Imaging of Quantum Dots Encapsulated in Phospholipid Micelles. *Science* **2002**, *298*, 1759–1762.

58 Platt, M.; Muthukrishnan, G.; Hancock, W. O.; Williams, M. E. Millimeter Scale Alignment of Magnetic Nanoparticle Functionalized Microtubules in Magnetic Fields. *J. Am. Chem. Soc.* **2005**, *127*, 15686–15687.

59 Grancharov, S. G.; Zeng, H.; Sun, S.; Wang, S. X.; O'Brien, S.; Murray, C. B.; Kirtley, J. R.; Held, G. A. Bio-functionalization of Monodisperse Magnetic Nanoparticles and Their Use as Biomolecular Labels in a Magnetic Tunnel Junction Based Sensor. *J. Phys. Chem. B* **2005**, *109*, 13030–13035.

60 Yu, W. W.; Chang, E.; Falkner, J. C.; Zhang, J.; Al-Somali, A. M.; Sayes, C. M.; Johns, J.; Drezek, R.; Colvin, V. L. Forming Biocompatible and Nonaggregated Nanocrystals in Water Using Amphiphilic Polymers. *J. Am. Chem. Soc.* **2007**, *129*, 2871–2879.

61 Robinson, D. B.; Persson, H. H. J.; Zeng, H.; Li, G.; Pourmand, N.; Sun, S.; Wang, S. X. DNA-Functionalized MFe_2O_4 (M = Fe, Co, or Mn) Nanoparticles and Their Hybridization to DNA-Functionalized Surfaces. *Langmuir* **2005**, *21*, 3096–3103.

62 Hutchins, B. M.; Platt, M.; Hancock, W. O.; Williams, M. E. Directing Transport of $CoFe_2O_4$-Functionalized Microtubules with Magnetic Fields. *Small* **2007**, *3*, 126–131.

63 Rosensweig, R. E. *Ferrohydrodynamics*; Dover, Mineola, NY, 1997.

64 (a) Vickrey, T. M.; Garcia-Ramirez, J. A. Magnetic Field-Flow Fractionation: Theoretical Basis. *Sep. Sci. Technol.* **1980**, *15*, 1297–1304. (b) Gorse, J.; Schunk, T. C.; Burke, M. F. The Study of Liquid Suspensions of Iron Oxide Particles with a Magnetic Field-Flow Fractionation Device. *Sep. Sci. Technol.* **1984–85**, *19*, 1073–1085.

65 Giddings, J. C.; Yang, F. J.; Myers, M. N. Flow-Field-Flow Fractionation: A Versatile New Separation Method. *Science* **1976**, *193*, 1244–1245.